

INTRACAVITY ABSORPTION OF He - Ne LASER  
RADIATION AS A DIRECT TIME-RESOLVED PROBE OF R + NO → RNO  
REACTION KINETICS (R = C<sub>3</sub>F<sub>7</sub>, CF<sub>3</sub>, CH<sub>3</sub>)

A B Vakhtin, A K Petrov

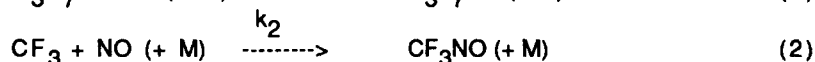
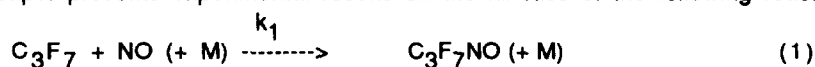
Institute of Chemical Kinetics and Combustion  
630090 Novosibirsk, USSR

**Abstract**

The reaction of NO with C<sub>3</sub>F<sub>7</sub>, CF<sub>3</sub> and CH<sub>3</sub> have been studied at room temperature using laser flash photolysis coupled with time-resolved product absorption. The pressure dependent rate coefficients were extrapolated using the Troe procedure to provide estimates of k<sub>0</sub> and k<sub>∞</sub>.

**1. Introduction**

This paper presents experimental results on the kinetics of the following reactions:



The kinetics of reaction (1) were studied for the first time. Data available in the literature on the kinetics of reactions (2)<sup>1-3</sup> and (3)<sup>4-6</sup> show some discrepancies. Most of the experimental results have been obtained in the fall-off pressure range and extrapolated, if at all, to low- and high-pressure limits to obtain k<sub>0</sub> and k<sub>∞</sub> ignoring the effect of weak collisions on the shape of the fall-off curves.

In the present work, we have studied the kinetics of reactions (1) - (3) at ambient temperature over a wide pressure range, (helium was used as a buffer gas). To construct theoretical fall-off curves and derive limiting values of k<sub>0</sub> and k<sub>∞</sub> we employed the Troe formalism<sup>7,8</sup> including procedures for calculation of k<sub>0</sub><sup>9</sup> and k<sub>∞</sub><sup>10,11</sup>.

**2. Experimental**

A pre-evacuated reaction cell was filled with a gas mixture (NO, radical precursor RI, buffer gas helium). Radicals were generated by pulsed photodissociation of the corresponding iodide by an excimer XeCl laser (λ = 308 nm, typical pulse energy, including losses = 10 mJ, repetition rate ca. 0.25 Hz). The kinetics of RNO accumulation were observed in real time on the microsecond time scale by the absorption of cw He-Ne laser radiation (λ = 632.8 nm) (absorption in the 600 - 700 nm range is a characteristic feature of nitroso compounds). The photolyzing and probing laser beams crossed in the cell at a small angle. The reaction cell was mounted inside the cavity of the He-Ne laser, enhancing the sensitivity by a factor of 150-200 as compared to linear absorption. The time resolution of the setup is ca. 2 -3 microseconds. The experiment was controlled and the kinetic data were derived and processed by a microcomputer. The absorption signal was digitized with a transient recorder (50 ns, 8 bits, 1024 words) and normalized to the photolyzing pulse energy. As a rule, each kinetic curve was averaged over 20 - 200 experimental runs.

**3. Results**

Fig. 1a shows a typical kinetic curve of RNO accumulation. Since the experiments were performed under conditions providing pseudo-first order reaction kinetics ([NO] >> [R]), the RNO concentration profiles are well described by the following function:

$$A(t) = A_0(1 - \exp(-t/\tau_r)) \cdot \exp(-t/\tau_d) \quad (i)$$

where  $\tau_r$  is the characteristic time of the reaction and  $\tau_d$  characterizes the product diffusion from the detection zone ( $\tau_r \ll \tau_d$ ).  $\tau_r$  is related to the pseudo-first order rate constant as follows:

$$1/\tau_r = k [\text{NO}]$$

Kinetic parameters were obtained from the kinetic curves by non-linear least squares.

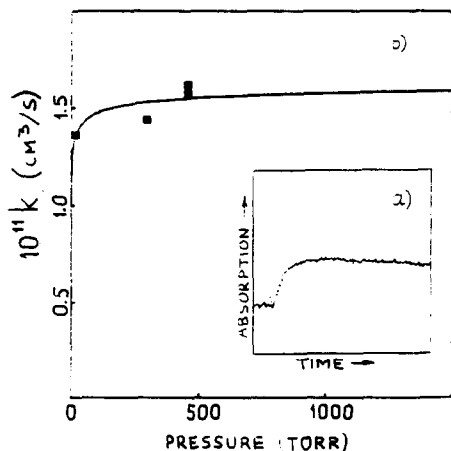


Fig. 1

- a) Typical absorption signal (photolysis of  $\text{C}_3\text{F}_7\text{I}$  and  $\text{CF}_3\text{I}$  in the presence of  $\text{NO}$ ).  
 b) Pressure dependence of the rate constant of reaction (1).

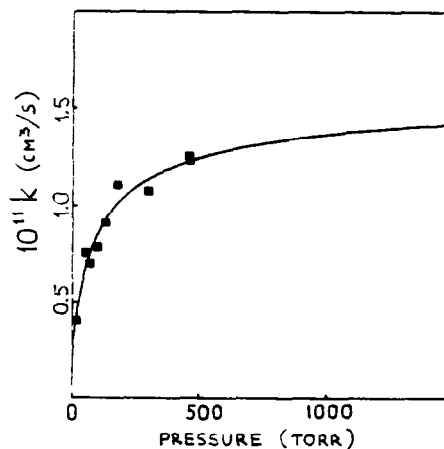


Fig. 2

- Pressure dependence of the rate constant of reaction (2).

Second-order rate constants were derived from linear plots of  $1/\tau_r$  vs  $[\text{NO}]$ . Reaction (1) is close to the high pressure limit under the experimental conditions (Fig. 1b) while reaction (2) is the fall-off regime (Fig. 2).

Fig. 3a shows examples of the kinetic curves obtained for the photolysis of  $\text{CH}_3\text{I}$  in the presence of  $\text{NO}$  which cannot be approximated by the equation (1). We resolved such kinetic curves into the sum of two exponentials:

$$A(t) = A_1(1 - \exp(-t/\tau_1)) + A_2(1 - \exp(-t/\tau_2)), \quad (ii)$$

the condition  $\tau_1 \ll \tau_2$  being met. Thus, besides the fast component corresponding to  $\text{CH}_3\text{NO}$  formation in reaction (3) there is a slow component which may be ascribed to the accumulation of molecular iodine by atom recombination.

It is necessary to explain the fact that we observed no  $\text{I}_2$  formation in experiments on the photolysis of  $\text{C}_3\text{F}_7\text{I}$  and  $\text{CF}_3\text{I}$ . This may be explained as follows. For an  $\text{I}_2$  molecule to be formed, two iodine atoms in the ground state  $^2P_{3/2}$  must recombine. It is known<sup>12,13</sup> that the photolysis of  $\text{CH}_3\text{I}$  at 308 nm yields mainly  $\text{I}(^2P_{3/2})$  while the photolysis of fluorinated alkyl iodides (in particular,  $\text{C}_3\text{F}_7\text{I}$  and  $\text{CF}_3\text{I}$ ) gives excited iodine atoms ( $^2P_{1/2}$ ), with close to unit efficiency, which do not undergo recombination and which relax very slowly. With  $\text{C}_3\text{F}_7\text{I}$  and  $\text{CF}_3\text{I}$ , therefore, no molecular iodine formation is expected on these timescales.

The rate constants of reaction (3) were derived from the slopes of the dependences of the reciprocal characteristic time of the fast component of the signal ( $1/\tau_1$ ), corresponding to  $\text{CH}_3\text{NO}$  accumulation, on  $\text{NO}$  concentration. Fig. 3b shows the pressure dependence of the rate constant of the reaction (3).

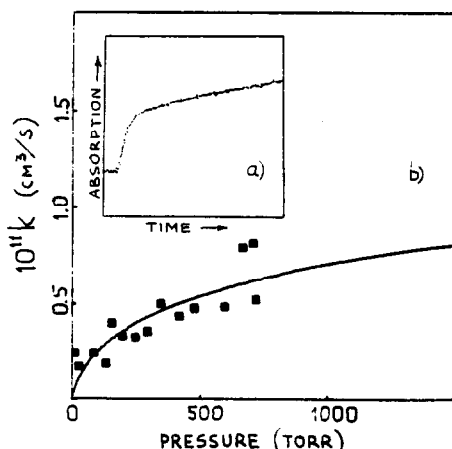


Fig. 3

- a) Typical absorption signal (photolysis of  $\text{CH}_3\text{I}$  in the presence of  $\text{NO}$ ).  
 b) Pressure dependence of the rate constant of reaction (3).

The limiting low- and high-pressure rate constants were obtained from experimental data by extrapolation of the fall-off curves  $k([M])$  to low and high pressures. To construct the fall-off curves we employed the approach developed by Troe et al.<sup>7,8</sup>. In terms of this approach the rate constant of the association/dissociation reaction is expressed in the form:

$$k/k_{\infty} = F_{\text{LH}} \cdot F_{\text{SC}} \cdot F_{\text{WC}} \quad (\text{iii})$$

where  $F_{\text{LH}} = \frac{k_0[M]/k_{\infty}}{1 + k_0[M]/k_{\infty}}$  is the well known expression of Lindemann-Hinshelwood,

$F_{\text{SC}}$  and  $F_{\text{WC}}$  are the two broadening factors.  $F_{\text{SC}}$  - the strong collision factor - corrects for the effect of the energy dependence of the microcanonical rate constant on the shape of the fall-off curve;  $F_{\text{WC}}$  - the weak collision factor - corrects for the effects of weak collisions.  $F_{\text{SC}}$  is a function of  $k_0[M]/k_{\infty}$  and of some properties of transition state, namely the average vibrational energy of the activated complex  $U^{\ddagger}_{\text{vib}}$ .  $F_{\text{WC}}$  is a function of  $k_0[M]/k_{\infty}$  and of the weak collision efficiency  $\beta_{\text{C}} = k_0/k_{0,\text{SC}}$ , where  $k_{0,\text{SC}}$  is the limiting low-pressure rate constant calculated in the strong collision approximation.

Theoretical curves  $k([M])$  for reactions (1 - 3) were constructed as follows. First, using an arbitrary value of  $U^{\ddagger}_{\text{vib}}$ , the best (iii) - type function was chosen by a non-linear least squares technique,  $k_0$  and  $k_{\infty}$  being employed as variable parameters. Note that  $k_0 = \beta_{\text{C}} \cdot k_{0,\text{SC}}$ .  $k_{0,\text{SC}}$  was calculated according to formulae proposed by Troe<sup>9</sup>. Then the  $U^{\ddagger}_{\text{vib}}$  value was estimated from the calculation of  $k_{\infty}$  by using the adiabatic channel model version for thermal rate constants<sup>10</sup> ( $\alpha/\beta$  was chosen to fit the current  $k_{\infty}$  value). This  $U^{\ddagger}_{\text{vib}}$  value was then used in the least-squares routine to obtain new  $k_0$  and  $k_{\infty}$  values. The procedure was repeated until the convergence was better than 5%.

The fall off curves obtained for reactions (1 - 3) and the main results are presented in figs. 1b, 2, 3b and in the table:

Reaction	$k_{0,\text{SC}}$ (Calc.) ----- cm <sup>6</sup> /s	$\beta_{\text{C}}$	$k_0$ ----- cm <sup>6</sup> /s	$k_{\infty}$ ----- cm <sup>3</sup> /s
$\text{C}_3\text{F}_7 + \text{NO} \rightarrow \text{C}_3\text{F}_7\text{NO}$	$3.2 \times 10^{-25}$	0.06	$2 \times 10^{-26}$	$1.76 \times 10^{-11}$
$\text{CF}_3 + \text{NO} \rightarrow \text{CF}_3\text{NO}$	$1.14 \times 10^{-27}$	0.038	$4.4 \times 10^{-29}$	$1.80 \times 10^{-11}$
$\text{CH}_3 + \text{NO} \rightarrow \text{CH}_3\text{NO}$	$3.7 \times 10^{-28}$	0.006	$2.2 \times 10^{-30}$	$1.7 \times 10^{-11}$

**4. References**

1. J.C. Amphlett, L.J. Macauley, *Can. J. Chem.*, 1976, v.54, p. 1234
2. K. Glanzer, M. Maier, J. Troe, *Chem. Phys. Letters*, 1979, v.61, p. 175
3. A.B. Vakhtin, A.K. Petrov, *Kinetika i Kataliz*, 1987, v.28, p. 1285 (in Russian)
4. H.E. Van den Bergh, A.B. Callear, *Trans. Faraday Soc.*, 1971, v.67, p. 2017
5. A.H. Laufer, A.M. Bass, *Int. J. Chem. Kinet.*, 1975, v.7, p.639
6. M.J. Pilling, J.A. Robertson, G.J. Rogers, *Int. J. Chem. Kinet.*, 1976, v.8, p. 833
7. J. Troe, *Ber Bunsenges. Phys. Chem.*, 1983, v.87, p. 161
8. R.G. Gilbert, K. Luther, J. Troe, *Ber. Bunsenges. Phys. Chem.*, 1983, v.87, p. 169
9. J. Troe, *J. Chem. Phys.*, 1977, v.66, p. 4758
10. J. Troe, *J. Chem. Phys.*, 1981, v. 75, p. 226
11. C.J. Cobos, J. Troe, *J. Chem. Phys.*, 1985, v.83, p. 1010
12. W.H. Pence, S.L. Baughcum, S.R. Leone, *J. Phys. Chem.*, 1981, v.85, p. 3844
13. E. Gerck, *J. Chem. Phys.*, 1983, v.79, p. 311